

LETTER TO THE EDITOR



Human SIDT1 mediates dsRNA uptake via its phospholipase activity

© The Author(s) under exclusive licence to Center for Excellence in Molecular Cell Science, Chinese Academy of Sciences 2023

Cell Research (2023) 0:1–4; <https://doi.org/10.1038/s41422-023-00889-x>

Dear Editor,

Systemic RNA interference (RNAi) refers to post-transcriptional gene silencing that spreads throughout the organism and its progeny, which could be triggered by double-stranded (ds) RNA.^{1,2} Hunter and colleagues identified that a ubiquitously expressed putative transmembrane protein SID-1 (systemic RNAi defective-1) in *Caenorhabditis elegans* is required for systemic RNAi,³ via acting as a channel to passively transport extracellular dsRNA into cells.^{4,5} SIDT1 (SID-1 transmembrane family member 1) is a SID-1 homolog in humans. Previous reports showed that it could facilitate the cellular uptake of both short interfering RNAs and microRNAs (miRNA).^{6–8} Given a sequence identity of ~24%, SIDT1 might function in a way similar to nematode SID-1. However, the molecular mechanism of either SID-1-mediated RNAi or SIDT1-facilitated dsRNA uptake remains unknown.

We purified human SIDT1 in glycol-diosgenin micelles, and solved its cryo-EM structure at 2.9 Å resolution (Supplementary information, Fig. S1). The overall structure of SIDT1 displays as a symmetric homodimer, each subunit of which contains two extracellular domains (ECDs), ECD1 and ECD2, in addition to a transmembrane domain (TMD) (Fig. 1a; Supplementary information, Fig. S2a). ECD1 is structurally similar to ECD2, both core structures of which fold into a two-layered β -sandwich consisting of four antiparallel β -strands in each layer (Fig. 1a; Supplementary information, Figs. S2a, S3a). Besides, ECD1 possesses an extra antiparallel β -hairpin that extends towards ECD2 (Fig. 1a). The TMD of SIDT1 comprises 11 helices (TM1–TM11), which resembles alkaline ceramidase and adiponectin receptor protein (Fig. 1a; Supplementary information, Fig. S3b). It structurally proved that SIDT1 is indeed a member of the superfamily CREST, in agreement with a previous bioinformatic prediction.⁹

In each subunit of SIDT1, a pair of disulfide bond Cys130–Cys220 and several non-covalent interactions lead to ECD1 being stabilized on ECD2, which further stacks on the TMD via interacting with a short α -helix_{772–778} and an extracellular loop_{TM2–TM3} (Supplementary information, Fig. S3c, d). Moreover, two SIDT1 subunits dimerize and form three interfaces (Fig. 1a), with a total buried interface area of 2698 Å². In detail, ECD1 interacts with ECD1' via four pairs of salt bridges and hydrogen bonds, whereas ECD2 forms a hydrophobic interface with ECD2' (Supplementary information, Fig. S3e, f). In addition, dimerization of TMD is maintained by hydrogen bonds and hydrophobic interactions contributed by TM2 and TM5 of each subunit (Supplementary information, Fig. S3g). These three interfaces make SIDT1 form a stable homodimer.

Further structural analysis enabled us to observe an extra density in the TMD of each SIDT1 subunit (Fig. 1a; Supplementary information, Fig. S4a), with a branched structure reminiscent of a phospholipid molecule. However, fitting the major components of membrane phospholipids with a hydrophilic headgroup yielded

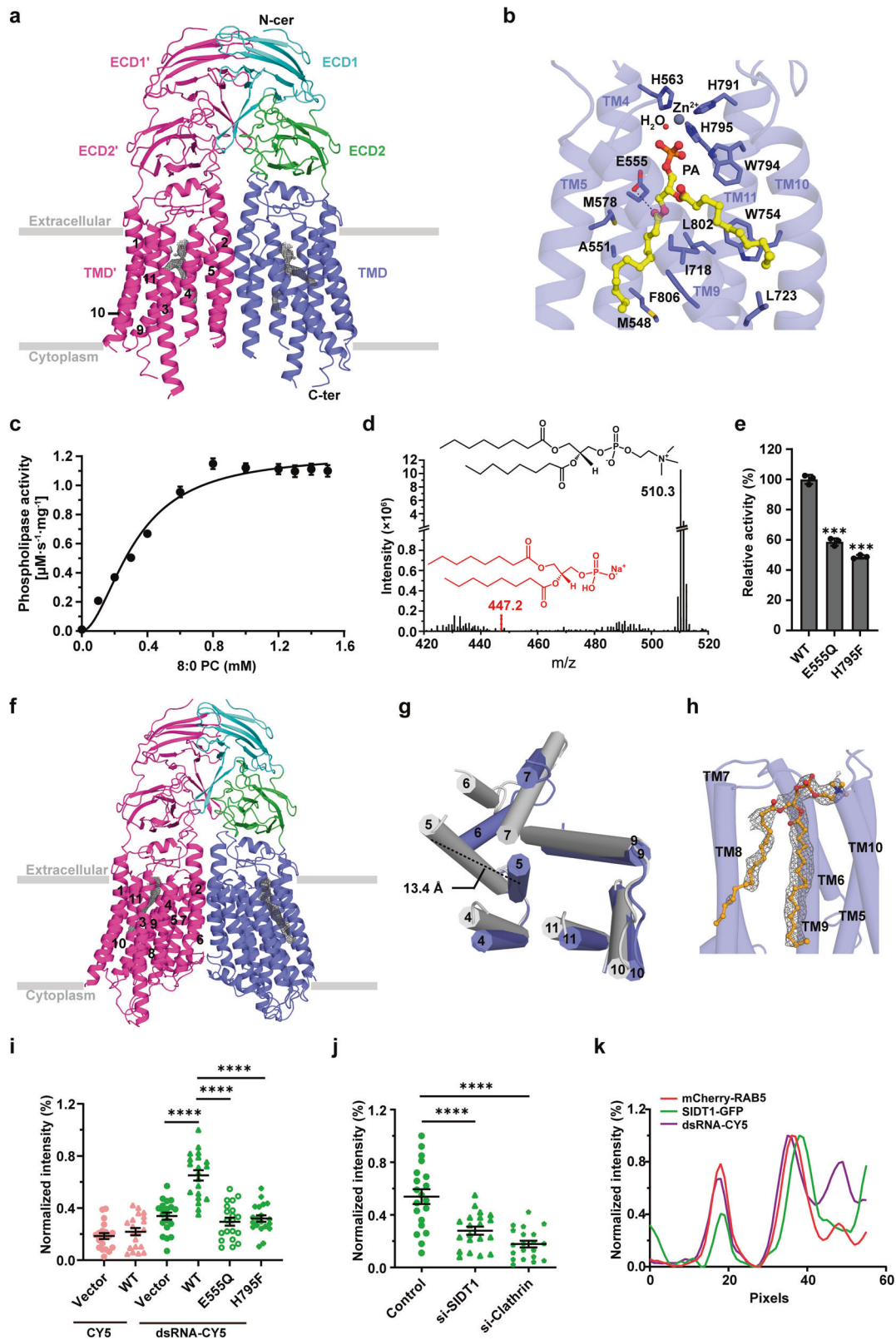
obvious steric clash with the residues His563, His791 and His795 surrounding the head of this extra density (Supplementary information, Fig. S4b). Finally, a 12-carbon phosphatidic acid (PA) molecule, a Zn²⁺ ion and a water molecule were perfectly fitted into the branched density (Supplementary information, Fig. S4b). The PA molecule is bound to a pocket surrounded by five TMs, via plenty of hydrophobic interactions in addition to the hydrogen bond between Glu555 from TM4 and the carbonyl group at one fatty acyl chain of PA (Fig. 1b). Multiple-sequence alignment revealed that most PA-binding residues are conserved in SIDT1 homologs (Supplementary information, Fig. S4c). Moreover, the putative Zn²⁺ ion is tetrahedrally coordinated by a water molecule and the side chains of the aforementioned three conserved histidine residues His563, His791 and His795 (Fig. 1b). A zoom-in superposition indicated that the Zn²⁺-coordination pattern of SIDT1 is nearly identical to the structure-known members of CREST superfamily (Supplementary information, Fig. S4d).

The presence of PA in our structure strongly indicated that SIDT1 might have the ability to cleave phospholipids at the distal phosphodiester bond, leaving one of the products PA in the catalytic pocket. Enzymatic activity assays showed that SIDT1 possesses the hydrolysis activity towards short-chain 8:0 phosphatidylcholine (PC), yielding a K_m of 323 μ M, and a V_{max} and K_{cat} of 1.2 μ M·s⁻¹·mg⁻¹ and 4.6 $\times 10^{-3}$ s⁻¹, respectively (Fig. 1c; Supplementary information, Fig. S5a). Mass spectrometry analysis of the reaction products enabled us to observe an additionally charged ion at $m/z = 447.2$, identical to that of 8:0 PA sodium salt plus one hydrogen atom (Fig. 1d; Supplementary information, Fig. S5b). Moreover, enzymatic activity assays revealed that the two single mutants E555Q and H795F exhibit a decrease of hydrolysis activity (Fig. 1e), suggesting that Glu555 (corresponding to Gln532 in SID-1) and His795 (conserved in SIDT1 homologs) might be necessary for product stabilization and substrate catalysis, respectively. Although DOPC could not be hydrolyzed due to its poor solubility, SIDT1 displayed a relatively low but detectable hydrolysis activity towards the long-chain DMPC and POPC (Supplementary information, Fig. S5a). Altogether, these results indicated that SIDT1 is a Zn²⁺-dependent transmembrane phospholipase D (PLD). The K_{cat} of SIDT1 is much lower than those of previously reported soluble or membrane-bound PLDs (e.g. ~5508 s⁻¹ for plant PLD, ~110 s⁻¹ for *Streptomyces klenkii* PLD and ~68 s⁻¹ for *Streptomyces hirosimensis* PLD).^{10–12} Notably, these PC hydrolases possess a large range of K_m value, from 18.9 μ M to 33 mM.^{10–12} In fact, it is reasonable that the transmembrane hydrolase SIDT1 possesses a rather low basal enzymatic activity towards the major component of cell membrane.

To obtain the substrate-complexed structure, we solved the structure of SIDT1 E555Q mutant (SIDT1^{E555Q}) at 2.4 Å (Supplementary information, Fig. S6). However, we failed in observing any EM density in the previously identified PA-binding pocket.

Received: 27 June 2023 Accepted: 14 October 2023

Published online: 06 November 2023



Notably, the three helices TM6–TM8, the side chains of which could not be assigned in the wild-type SIDT1, were finely modeled in the final map of SIDT1^{E555Q} (Fig. 1f; Supplementary information, Fig. S2b). Structural superposition revealed that the ECDs could be well aligned, but the TMDs undergo obvious conformational changes (Supplementary information, Fig. S7a). Especially, TM5 of

SIDT1^{E555Q} moves ~13.4 Å inwards towards the PA-binding pocket, resulting in the collapse of the binding pocket (Fig. 1g; Supplementary information, Fig. S7b). In addition, Asp574 from TM5, a conserved residue in members of CREST superfamily,⁹ participates in the Zn²⁺-coordination with three histidine residues (Supplementary information, Fig. S7c). Moreover, we found an

Fig. 1 Structures of human SIDT1 and its phospholipase activity-dependent dsRNA uptake. **a** Cartoon representation of wild-type SIDT1 complexed with PA. One subunit is colored in magenta, whereas the other subunit is labeled in different colors to show major domains: ECD1 (cyan), ECD2 (green) and TMD (blue). Two extra densities, each of which could accommodate a PA molecule, are shown as the black mesh. Transmembrane helices (TMs) are labeled, except for the helices TM6 to TM8. **b** The PA-binding pocket. The PA molecule is shown as yellow stick, whereas the Zn²⁺ ion and H₂O are shown as gray and red spheres, respectively. The hydrophobic residues surrounding two fatty acid chains within 4 Å and the Zn²⁺-coordinated residues are shown as sticks and labeled. The hydrogen bond is indicated as black dotted line. **c** The phospholipase activity of SIDT1 upon addition of the 8:0 phosphatidylcholine (PC) at various concentrations. Each data point is the average of three independent experiments ($n = 3$), and error bars represent the means \pm SD. The data points were fitted with a Hill equation. **d** Mass spectrum of SIDT1 plus the 8:0 PC sample. Additional signal for the 8:0 PA is colored in red. The charged ion at $m/z = 447.2$ corresponds to 8:0 PA sodium salt plus one hydrogen atom, whereas that of 510.3 is 8:0 PC plus one hydrogen atom. **e** Relative phospholipase activities of SIDT1 and mutants towards the 8:0 PC. *** $P < 0.001$ by one-way ANOVA. **f** Cartoon representation of SIDT1^{E555Q}. The color scheme is the same as wild-type SIDT1. Two extra densities, each of which could be fitted with a POPC molecule, are shown as the black mesh. **g** Superposition of TMs with conformational changes of the wild-type SIDT1 (gray) against SIDT1^{E555Q} (blue) in a view from the cytoplasm. The distance between the C α atoms of Thr592 on TM5 within two structures is labeled. **h** The hydrophobic POPC-binding pocket. The density of the POPC molecule is shown in gray mesh, and contoured at 4 σ . **i, j** Statistical analyses against the uptake of Cy5 and dsRNA-Cy5 in HEK293T cells transfected with **(i)** GFP vector, wild-type SIDT1 (WT) or mutant (E555Q/H795F) plasmid, and **(j)** SIDT1 or Clathrin siRNA. $n = 20$, which represents the number of transfected cells from three independent experiments. Data represent means \pm sem. Ordinary one-way ANOVA followed by Tukey's post hoc test was used to determine statistical significance. **** $P < 0.0001$. **k** Colocalization of SIDT1 with the early endosome (RAB5 as marker) upon dsRNA-Cy5 treatment. Line scan analysis across indicated lines of the representative image was performed to assess relative colocalization.

extra density at the lateral of TMD of SIDT1^{E555Q}, which could be fitted with a POPC molecule (Fig. 1h; Supplementary information, Fig. S6). It lies in the hydrophobic cleft composed of TM8–TM10, and forms hydrogen bond and π -cation interaction with Asn764 from TM9 and Phe761 from TM10, respectively (Supplementary information, Fig. S7d). It is possible that the substrate might enter the catalytic pocket via a lateral access path.

Structural analyses indicated that the cellular uptake of dsRNA is dependent on the PLD activity of SIDT1. Accordingly, a series of fluorescence assays were performed to verify this hypothesis. In the cells that overexpress SIDT1, the cellular uptake of Cy5 alone was not observed, whereas that of Cy5-labeled dsRNA is significantly increased compared to the control transfectant (Fig. 1i; Supplementary information, Fig. S8a). In contrast, knock-down of *sdit1* gene significantly attenuated the uptake of dsRNA (Fig. 1j; Supplementary information, Fig. S8b, c), which supported that SIDT1 is involved in the uptake of extracellular dsRNA into cells. Moreover, the statistical analysis of fluorescence intensities showed that the uptake of dsRNA is decreased to a half in the cells that overexpress either E555Q or H795F mutant, compared to that in the wild-type SIDT1 transfectant (Fig. 1i; Supplementary information, Fig. S8a, d). These results suggested that the phospholipase activity plays an important role in SIDT1-mediated uptake of dsRNA. Furthermore, knock-down of *Clathrin*, which encodes a protein participating in endocytosis,¹³ also impaired the uptake of dsRNA (Fig. 1j; Supplementary information, Fig. S8b, c). Meanwhile, fluorescence co-localization assays revealed that SIDT1 co-localizes with the early endosome in the presence of dsRNA (Fig. 1k; Supplementary information, Fig. S8e). Thus we proposed that the phospholipase activity of SIDT1 generates the major hydrolysate PA, which introduces a negative curvature of the lipid bilayer to facilitate the fission and fusion of membranes.¹⁴ This property would enable SIDT1 to initiate an dsRNA uptake pathway via trimming the membrane phospholipids.

In addition, fluorescence uptake assays were also performed against miRNA and dsDNA. The results revealed that the wild-type SIDT1 could facilitate their cellular uptake, which is also impaired in the cells that overexpress either E555Q or H795F mutant (Supplementary information, Fig. S9). It suggested that SIDT1-mediated uptake of various nucleotides is most likely dependent on its phospholipase activity. Moreover, we found a similar cellular uptake rate at pH 7.2 and pH 4.5 (Supplementary information, Fig. S9), which is consistent with the data of a previous report.⁸ However, we did not prove the dramatic enhance of miRNA uptake in the medium at the very low pH values, such as 4.0 and

3.5, which is a major conclusion of the previous SIDT1 work using the primary gastric epithelial cells,⁸ as the HEK293T cells could not survive in such acidic medium.

In summary, we report the PA-bound structure of human SIDT1, the TMD of which indeed possesses the core structure of members in the CREST superfamily,⁹ but functions as a homodimer and adopts a reversed topology (Supplementary information, Fig. S10). Structural analysis combined with biochemical assays indicate that SIDT1 is a transmembrane phospholipase towards PC, which further proves that the majority of CREST members are putative hydrolases. However, SIDT1 is structurally distinct from the previously reported soluble or membrane-bound PLDs. Furthermore, a series of fluorescence assays suggest that SIDT1 mediates the uptake of either dsRNA, miRNA or dsDNA, via the phospholipase activity. These findings not only advance the understanding of both CREST and PLD superfamilies, but also enable us to identify a clade of transmembrane phospholipase and an uptake pathway via trimming the membrane phospholipids.

Recently, a group reported the structure of human SIDT2,¹⁵ which is also a homolog of SID-1 and shares a primary sequence identity of 58% with SIDT1. The apo-form structure of SIDT2 is much similar to our structure of SIDT1^{E555Q} (Supplementary information, Fig. S11). Moreover, we purified human SIDT2 in detergent micelles and applied it to enzymatic activity assays. The results showed that SIDT2 could also hydrolyze the 8:0 PC (Supplementary information, Fig. S12), with a K_m , V_{max} and K_{cat} of 352 μ M, 1.2 μ M \cdot s⁻¹ \cdot mg⁻¹ and 2.3 $\times 10^{-3}$ s⁻¹, respectively, which are comparable to those of SIDT1.

Notably, another accompanying paper revealed that the ECDs of SIDT1 and SIDT2 bind dietary miRNAs only under acidic conditions, which could further trigger the higher-order oligomerization of both proteins. The authors thus proposed a low pH-dependent activation for small RNA uptake mediated by SIDT1 and SIDT2. However, further investigations are needed to identify the potential agonist or partner protein(s) of SIDT1, which is necessary for its optimal activity.

Cai-Rong Sun^{1,2,7}, Da Xu^{1,2,7}, Fengrui Yang^{3,7}, Zhuanghao Hou⁴, Yuyao Luo⁵, Chen-Yu Zhang⁶, Ge Shan^{1,2,7}, Guangming Huang^{1,2,7}, Xuebiao Yao^{3,7}, Yuxing Chen^{1,2,7}, Qiong Li^{1,2,7} and Cong-Zhao Zhou^{1,2,7}

¹School of Life Sciences, Division of Life Sciences and Medicine, University of Science and Technology of China, Hefei, Anhui, China.

²Biomedical Sciences and Health Laboratory of Anhui Province, University of Science and Technology of China, Hefei, Anhui, China.

³MOE Key Laboratory for Cellular Dynamics, University of Science and Technology of China, Hefei, Anhui, China. ⁴School of Chemistry and Materials Science, National Synchrotron Radiation Laboratory, University of Science and Technology of China, Hefei, Anhui, China. ⁵Department of Clinical Laboratory, The First Affiliated Hospital of USTC, Hefei National Laboratory for Physical Sciences at Microscale, the CAS Key Laboratory of Innate Immunity and Chronic Disease, School of Basic Medical Sciences, Division of Life Science and Medicine, University of Science and Technology of China, Hefei, Anhui, China. ⁶Nanjing Drum Tower Hospital Center of Molecular Diagnostic and Therapy, State Key Laboratory of Pharmaceutical Biotechnology, Jiangsu Engineering Research Center for MicroRNA Biology and Biotechnology, NJU Advanced Institute of Life Sciences (NAILS), School of Life Sciences, Nanjing University, Nanjing, Jiangsu, China. ⁷These authors contributed equally: Cai-Rong Sun, Da Xu, Fengrui Yang. ✉email: yaoxb@ustc.edu.cn; cyxing@ustc.edu.cn; liqiong@ustc.edu.cn; zcz@ustc.edu.cn

DATA AVAILABILITY

All relevant data are available from the authors and/or included in the manuscript or Supplementary information. The cryo-EM structures of wild-type SIDT1 complexed with PA and SIDT1^{E555Q} have been deposited at PDB under the codes of 8JUL and 8JUN, respectively. The cryo-EM density maps of two structures have been deposited at the Electron Microscopy Data Bank under accession codes: EMD-36661 for PA-bound SIDT1, and EMD-36662 for SIDT1^{E555Q}.

REFERENCES

1. Fire, A. et al. *Nature* **391**, 806–811 (1998).
2. Tabara, H., Grishok, A. & Mello, C. C. *Science* **282**, 430–431 (1998).
3. Winston, W. M., Molodowitch, C. & Hunter, C. P. *Science* **295**, 2456–2459 (2002).
4. Feinberg, E. H. & Hunter, C. P. *Science* **301**, 1545–1547 (2003).
5. Shih, J. D. & Hunter, C. P. *RNA* **17**, 1057–1065 (2011).
6. Duxbury, M. S., Ashley, S. W. & Whang, E. E. *Biochem. Biophys. Res. Commun.* **331**, 459–463 (2005).
7. Wolfrum, C. et al. *Nat. Biotechnol.* **25**, 1149–1157 (2007).
8. Chen, Q. et al. *Cell Res.* **31**, 247–258 (2021).
9. Pei, J., Millay, D. P., Olson, E. N. & Grishin, N. V. *Biol. Direct* **6**, 37 (2011).
10. Li, J. et al. *Cell Res.* **30**, 61–69 (2020).
11. Hu, R., Cui, R., Lan, D., Wang, F. & Wang, Y. *Int. J. Mol. Sci.* **22**, 10580 (2021).
12. Li, C., Xia, Y., Li, M. & Zhang, T. *Heliyon* **8**, e12587 (2022).
13. Kaksonen, M. & Roux, A. *Nat. Rev. Mol. Cell Biol.* **19**, 313–326 (2018).
14. Kooijman, E. E. et al. *Biochemistry* **44**, 2097–2102 (2005).
15. Qian, D. et al. *Nat. Commun.* **14**, 3568 (2023).

ACKNOWLEDGEMENTS

We thank Dr. Yong-Xiang Gao for technical support on cryo-EM data collection at the Cryo-EM Center at the University of Science and Technology of China (USTC). This work was supported by the Strategic Priority Research Program of the Chinese Academy of Sciences (XDB37020202) and Research Funds of Center for Advanced Interdisciplinary Science and Biomedicine of IHM (QYZD20220001).

AUTHOR CONTRIBUTIONS

C.Z.Z., Y.C. and Q.L. conceptualized and supervised the project. C.R.S., D.X. and Q.L. designed all the experiments. C.Y.Z. provides the plasmid encoding SIDT1. C.R.S. performed cloning, expression, purification and cryo-EM sample preparation. C.R.S. and D.X. performed cryo-EM data collection, structure determination and model refinement. C.R.S. performed phospholipase activity assays. Z.H. and G.H. performed mass spectrometry analyses. F.Y., X.Y., Y.L. and G.S. performed fluorescence experiments and data analyses. Q.L., C.R.S., C.Z.Z. and Y.C. wrote the manuscript.

COMPETING INTERESTS

The authors declare no competing interests.

ADDITIONAL INFORMATION

Supplementary information The online version contains supplementary material available at <https://doi.org/10.1038/s41422-023-00889-x>.

Correspondence and requests for materials should be addressed to Xuebiao Yao, Yuxing Chen, Qiong Li or Cong-Zhao Zhou.

Reprints and permission information is available at <http://www.nature.com/reprints>